Self-Propelled Droplet Removal from Hydrophobic Fiber-Based Coalescers: Supplemental Material

Kungang Zhang,[1] Fangjie Liu,[1] Adam J. Williams,[1] Xiaopeng Qu,[1] James J. Feng,[2,3] and Chuan-Hua Chen[1*]

[1]*Department of Mechanical Engineering and Materials Science, Duke University, Durham, NC 27708, USA*
[2]*Department of Mathematics, University of British Columbia, Vancouver, BC, Canada V6T 1Z2 and*
[3]*Department of Chemical and Biological Engineering,*
University of British Columbia, Vancouver, BC, Canada V6T 1Z3
(Dated: July 2, 2015)

Contents

---

*Electronic address: chuanhua.chen@duke.edu

S1. EXPERIMENTAL METHODS

The experimental methods are described in this section for the self-removal process on fiber-based coalescers (Fig. S1a) and the coalescence-induced launching mechanism (Fig. S1b). Unless otherwise specified, all the fibers are coated with a thin layer of teflon by dip coating (DuPont AF2400) followed by baking at $130°$C for 15 minutes. The teflon coating exhibits advancing and receding contact angles of $121 \pm 3°$ and $108 \pm 2°$, respectively, as measured on a flat copper surface treated with the same coating procedure.
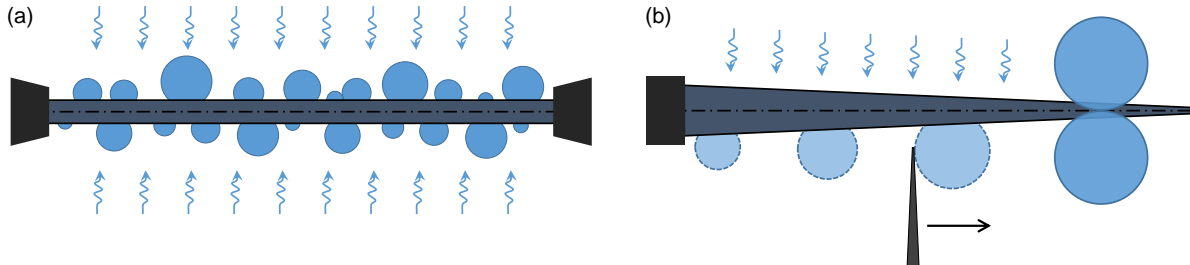

FIG. S1: Experimental setup: (a) Constant-radius fiber used to study the long-term condensation process in Fig. 1; (b) Conical fiber used to study the rapid coalescence and launching process in Fig. 2.

A. Condensation process on fibers

The condensation process is studied on teflon-coated fibers with a uniform radius (Fig. S1a). The fibers are cooled below the dew point to induce condensation of the water vapor in the ambient air. In Fig. 1(a-c), a $40 \, \mu$m-radius, 8.1 mm-long copper fiber (McMaster-Carr 40AWG) is held at both ends by solid supports that are cooled to $7°$C, and the ambient air is at $25°$C with a humidity of 49%. (Note that the exact thermal conditions are not essential for this study and may fluctuate from experiment to experiment.) The condensation process is recorded by video imaging at 5 frames per second (fps) initially and 2 fps at large times, using a long-distance microscope (Infinity K2) and a Pixelfly QE camera. The process is initialized by removing the accumulated condensate from the fiber with a nitrogen gun, and time 0 is assigned to the frame immediately preceding the first reappearance of condensate drops. In Fig. 1(d), the condensate growth is also studied on a $13 \, \mu$m-radius gold fiber (California Fine Wire 0.001in), again with teflon coating.

B. Coalescence-induced launching on fibers

The coalescence and subsequent launching of two symmetric drops are studied on teflon-coated conical fibers (Fig. S1b). A cone is produced by gradually pulling a $255 \, \mu$m-radius copper fiber (McMaster-Carr 24AWG) from 18%wt nitric acid.[1] With a retracting speed of 1 mm/s controlled by a motorized stage (Oriental Motor PK564NAW), a smooth cone is produced with an apex angle of $4°$. The copper cone is then coated with teflon using the aforementioned procedure. The conical fiber is cooled at the base to induce condensation from the ambient air toward the cone, permitting the endview from the free tip. The conical fiber is visualized from both the end and the side, with the optical axis parallel and perpendicular to the axial direction, respectively. The end and side views are simultaneously captured via K2 microscopes with Phantom 710 and 7.1 high-speed cameras, respectively. Time 0 is assigned to the frame immediately preceding the coalescence, which is initiated by gentle perturbation of the drops. The launching velocity is extracted from the trajectory of the launched drop while accounting for the influence of gravity.[2] Since only the "center of mass" of the projected 2D images can be tracked, a long trajectory of at least several drop diameters is used to ensure accurate measurements.

In the coalescence experiments schematically shown in Fig. S1b, a condensate drop of desired radius is first identified on the conical fiber. A maneuvering probe is used to clean unnecessary drops blocking the end view, and then to move a

---

[1] É. Lorenceau, D. Quéré, J. Fluid Mech. **510**, 29 (2004).
[2] F. Liu, G. Ghigliotti, J. J. Feng, C.-H. Chen, J. Fluid Mech. **752**, 22 (2014).

second condensate drop toward the same axial location as the first one. Unless otherwise specified, all coalescences are symmetric between two drops of nearly identical radii (within 6% of the average drop radius r_d). Prior to coalescence, two drops are situated such that the line connecting the centers of mass is orthogonal to the axial direction. The drop coalescence is then induced by a gentle azimuthal movement of the second drop by the maneuvering probe. The average drop radius (r_d) is varied by judicious selection of the first drop, occasionally aided by the maneuvering probe that sweeps a few condensate drops along the fiber toward the drops of interest. The fiber radius (r_f) is varied by selecting the axial location of drop coalescence on the conical fiber, which has a small apex angle and therefore mildly varying radius along the fiber. The tip of the maneuvering probe is used to minimize the interference to the drop coalescence process, and the tip radius is always much smaller than the local radius (r_f) of the conical fiber. Both r_d and r_f are measured in the side view since the base of the conical fiber blocks part of the end view.

C. Control experiments and parametric variations

Geometrical configuration: In the coalescence experiments depicted in Fig. S1b, two drops are situated on the opposite sides of a fiber (Fig. S2a). As control cases, coalescence processes are studied with the drop situated on the same side of the fiber (Fig. S2b) and also on a flat substrate (Fig. S2c). Drop coalescence on the same side of the fiber (Fig. S2b) is investigated with nearly identical procedure as described in the previous subsection. For coalescence on either the same side or the opposite sides, the relative position of the drops with respect to the fiber is controlled by the maneuvering probe. The control case on a flat teflon substrate (Fig. S2c) is studied on polytetrafluoroethylene (PTFE) thread sealant tape (Mil Spec T27730A) attached to a rigid glass substrate. To minimize gravitational effects, small drops are produced by accumulation of inkjet-printed droplets. The inkjet nozzle with a radius of $20\,\mu m$ (MicroFab MJ-AL-01-40-8MX) is controlled by a function generator (Agilent 33220A) via a high-voltage amplifier (A. A. Lab A-301HS). Drop coalescence is triggered by the perturbation of an incoming printed droplet.

Drop and fiber radii: An upper bound on r_d is imposed by the gravitational limit, and a lower bound on r_f is imposed by the stiffness of the fiber as well as the finite size of the maneuvering probe. For drop coalescence with large radius ratios, typically with $r_d/r_f \gtrsim 10$, the merged drop can occasionally "wrap" around the fiber (see Fig. S6 below). Unless otherwise specified, all cases with visible wrapping have been excluded from the velocity data. When asymmetric coalescence between a larger drop (r_d) and a smaller drop (r_d') is studied, both drops are maneuvered such that the line connecting the centers of mass is still approximately orthogonal to the axial direction.

Surface wettability: In addition to the teflon coating used for the majority of the experiments, other coating materials are employed to test the dependence on wettability. The copper fibers are alternatively coated with either a monolayer of alkylthiol or a thin film of polystyrene. For alkylthiol coating, the conical copper fiber fresh from acid etching is treated with a $2\,mM$ solution of 1-hexdecanethiol (Acros AC12052-0100) in ethanol. The alkylthiol coating exhibits advancing and receding contact angles of $110 \pm 4°$ and $74 \pm 9°$, respectively. For polystyrene coating, the copper fiber is dip-coated in 2%wt polystyrene (Sigma Aldrich 182427) dissolved in toluene. The polystyrene coating exhibits advancing and receding contact angles of $93 \pm 4°$ and $68 \pm 3°$, respectively.
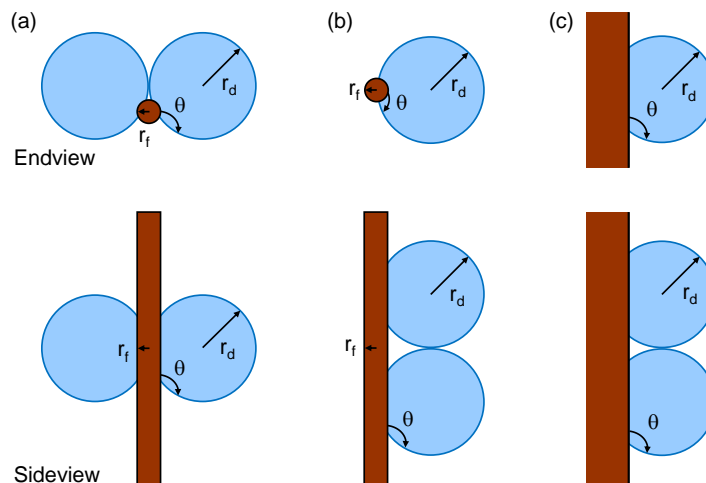

FIG. S2: Geometrical configuration for coalescence of two identical drops on a solid support: (a) Coalescence on opposite sides of a fiber; (b) Coalescence on the same side of a fiber; (c) Coalescence on a flat substrate. In addition to the geometrical dependence, the symmetric coalescence depends on the drop radius r_d, the fiber radius r_f and the Young's contact angle θ.

S2.   DEPENDENCE ON GEOMETRICAL CONFIGURATION
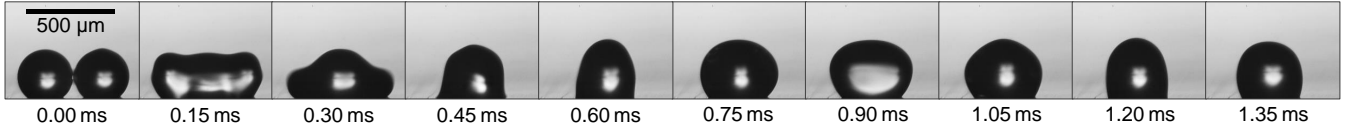
A.   Coalescence process on a flat substrate

FIG. S3: Coalescence process on a flat teflon substrate (Fig. S2c), on which self-launching does not occur. Gravity points downward. The average drop radius is $154\,\mu$m. See also Video S7.
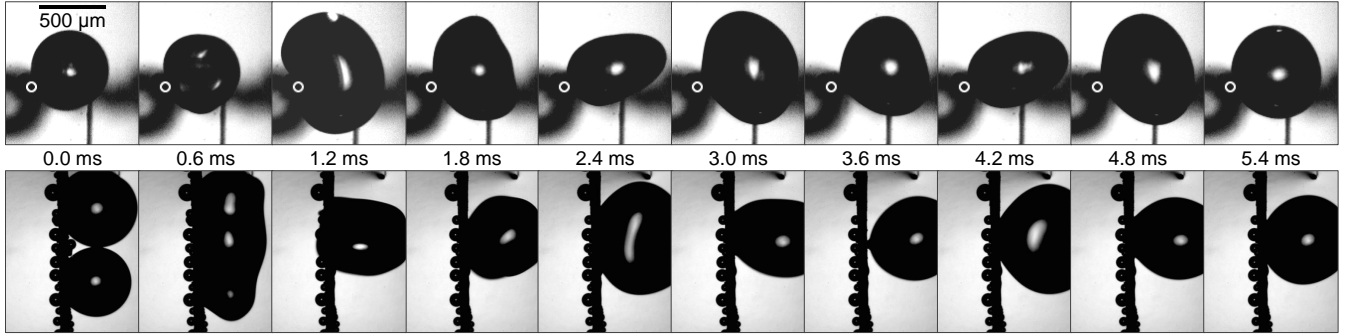
B.   Coalescence process on the same side of a fiber

FIG. S4: Coalescence process on the same side of a teflon-coated fiber (Fig. S2b). The top and bottom rows are the end and side views (not aligned), respectively. The average drop radius $r_d = 275\,\mu$m and the fiber radius $r_f = 35\,\mu$m. Gravity points rightward. For same-side coalescences, the drop-to-fiber radius ratio of $r_d/r_f = 7.8$ is around the threshold for the self-launching, evident from the near detachment at 3.6 ms. See also Video S8.

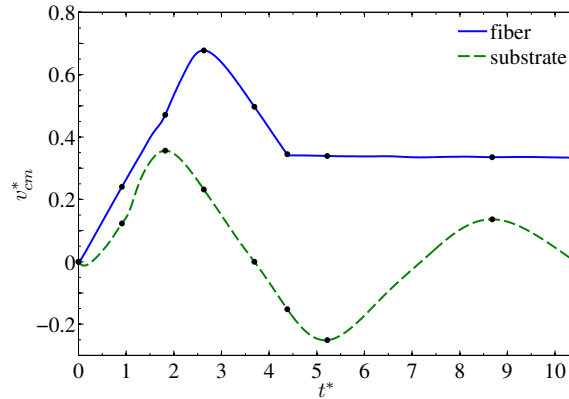## C.   Simulated velocity evolution on a fiber versus a substrate

FIG. S5: Simulated center-of-mass velocity of the merged drop as a function of time, corresponding to Fig. 3 where the velocity fields are captured at the time stamps (dots) indicated in the $v_{cm}^*(t^*)$ curves. Except for the presence of the three-phase contact lines with a mobility $\gamma^* = 10^{-3}$, all other parameters including the fluid properties at 20°C adopt those in Liu et al.[3] The 2D simulations indicate that the fiber case in Fig. S2a is conducive to self-launching, while the substrate case in Fig. S2c prohibits such spontaneous detachment.

[3] F. Liu, G. Ghigliotti, J. J. Feng, C.-H. Chen, J. Fluid Mech. **752**, 39 (2014).

S3. DEPENDENCE ON DROP AND FIBER RADII

A. Wrapping effect at large drop-to-fiber radius ratios
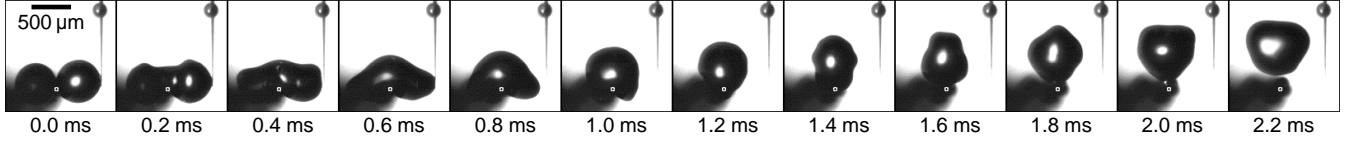

FIG. S6: The merged drop wraps around a teflon-coated fiber prior to the eventual self-launching. The wrapping occurs at approximately 1.2 ms, when the two wave rests merge in the back of the fiber. Gravity points leftward. The average drop radius $r_d = 262\,\mu$m and the fiber radius $r_f = 18\,\mu$m ($r_d/r_f = 15$). See also Video S9.

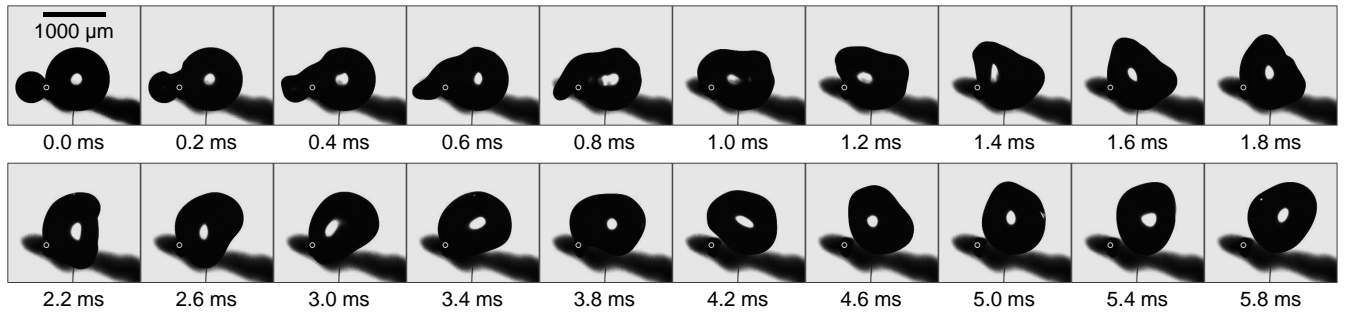### B. Asymmetric coalescence with unequal drop radii

FIG. S7: Asymmetric coalescence between drops of unequal radii on a teflon-coated fiber. The asymmetry gives rise to a significant rotational motion accompanying the self-propelled launching at approximately 3.8 ms. Gravity points rightward. The larger drop radius $r_d = 507\,\mu$m, the smaller drop radius $r_d' = 254\,\mu$m, and the fiber radius $r_f = 39\,\mu$m ($r_d'/r_d = 0.50$, $r_d'/r_f = 6.5$). See also Video S10.

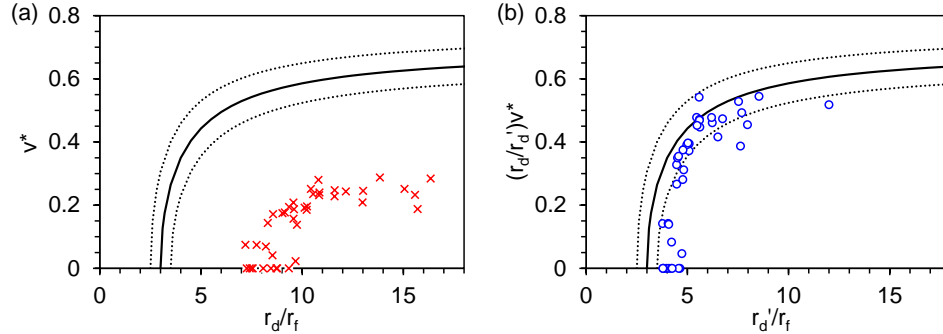### C. Launching velocity of asymmetric coalescences

FIG. S8: Launching velocity upon asymmetric drop coalescence between a larger drop (r_d) and a smaller drop (r_d') on teflon-coated fibers with $r_d'/r_d = 0.51 \pm 0.03$: (a) The data is plotted according to $\rho r_d^3 v^2 = c_1 \sigma r_d^2 - c_2 \sigma r_d r_f$ in Eq. (1); (b) The data is recast according to $\rho r_d^3 v^2 = c_1 \sigma r_d'^2 - c_2 \sigma r_d' r_f$ with the same prefactors. The nondimensional velocity $v^* = v/u_{ci}$, where $u_{ci} = \sqrt{\sigma/(\rho r_d)}$ as in the main text. The solid line is the same as the semi-empirical relationship in Fig. 4(c), and the dotted lines are uncertainty bounds in accordance with $v_\infty^* = 0.7 \pm 0.05$ and $\Gamma_{cr} = 3 \pm 0.5$. The reasonable fitting in (b) suggests that the launching velocity of asymmetric coalescence approximately scales as $(r_d'/r_d)u_{ci}$, and the critical condition for launching is roughly governed by $r_d'/r_f > \Gamma_{cr}$.

S4.   DEPENDENCE ON SURFACE WETTABILITY

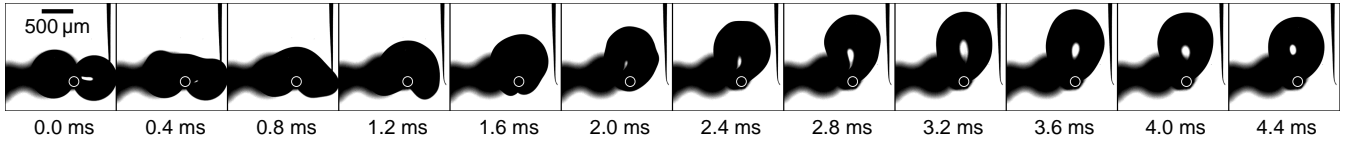### A.   Coalescence process on polystyrene-coated fibers

FIG. S9: Drop coalescence on a polystyrene-coated fiber does not give rise to self-launching. Gravity points leftward. The average drop radius $r_d = 360\,\mu$m and the fiber radius is $r_f = 76\,\mu$m ($r_d/r_f = 4.7$). See also Video S11.
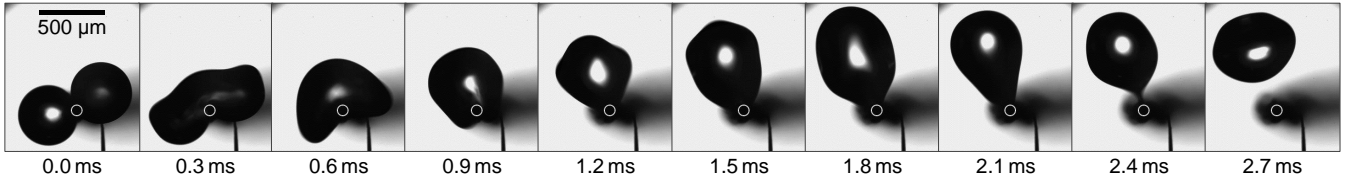
B.   Self-launching on alkylthiol-coated fibers

FIG. S10: Self-launching process from an alkylthiol-coated fiber. Gravity points rightward. The average drop radius $r_d = 238\,\mu$m and the fiber radius $r_f = 44\,\mu$m ($r_d/r_f = 5.4$). Compared to teflon-coated fiber, the alkylthiol-coated fiber has a lower contact angle and a larger hysteresis, giving rise to a prolonged snap-off process after which a tiny residual drop is left behind. See also Video S12.

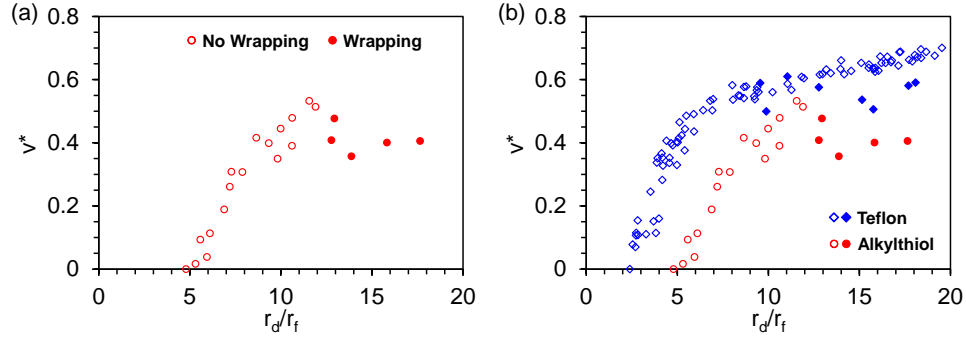### C.   Launching velocity on alkylthiol-coated fibers

FIG. S11: Launching velocity upon symmetric drop coalescence: (a) On alkylthiol-coated fiber, on which wrapping occurs consistently when the radius ratio r_d/r_f is above 12 or so; (b) Comparison with teflon-coated fiber using the $r_f = 25$–$35\,\mu$m data series in Fig. 4(c). For both coatings, the wrapping around the fiber (filled symbols) can significantly reduce the nondimensional launching velocity v^*.